A Vision Based Bio-Cell Recognition for Biomanipulation with Multiple Views

Min Soo Jang*, Seok Joo Lee*, Ho Dong Lee*, Byungkyu Kim**, Jong-Oh Park** and Gwi Tae Park*

* Department of Electrical Engineering, Korea University, Seongbuk Gu, Seoul 407, Korea
(Tel: 82-2-3290-3673; Fax: 82-2-953-3673; E-mail: {jangms, gidung, juragic, gtpark}@elec.korea.ac.kr)
**Microsystem Research Center, Korea Institute of Science and Technology, P.O.BOX 131, Cheongryang, Seoul, Korea
(Tel: 82-2-958-6819; E-mail: {bkim, jop}@kist.re.kr)

Abstract: Manipulation of the nano/micro scale object has been a key technology in biology as the sizes of DNA, chromosome, nucleus, cell and embryo are within such order. For instance, for embryo cell manipulation, the cell injection is performed manually. The operator often spends over a year to carry out a cell manipulation project. Since the typical success rate of such operation is extremely low, automation of such biological cell manipulation has been asked.

As the operator spends most of his time in finding the position of cell in the Petri dish and in injecting bio-material to the cell from the best orientation. In this paper, we propose a new strategy and a vision system, by which one can find, recognize and track nucleus, polar body, and zona pellucida of the embryo cell for automatic biomanipulation. The deformable template matching algorithm has been used in recognizing the nucleus and polar body of each cell. Result suggests that it outperforms the conventional methods.

Keywords: Biomanipulation, Bio-Cell Recognition, Deformable Template, Multiple Views

1. Introduction

Recently, manipulating the objects within the nano/micro scale is a key technology in biology, since the sizes of DNA, chromosome, nucleus, cell and embryo are within the order of nano/micrometer [1-4]. However, such manipulation is typically very difficult, simply because the objects are very weak, small (e.g. mouse embryo 1um – 40um), and the operation should be accomplished in the culture fluid.

And yet, most of the cell manipulations are carried out manually. Therefore, the operators should spend over a year to perform reliable cell manipulation. Since they depend on visual inspection, the success rate and efficiency of manipulation is extremely low because of eyestrain. For such reason, automation of biomanipulation is necessary

In case of the embryo cell manipulation, the insertion position of a pipette is mainly determined by arrangement of inner structure of the cell. So, in conventional biomanipulation system, the operator spends most of his time in finding the position of the cell in the petri dish and recognizing the best orientation for injecting bio-material to the cell.

In this paper, we propose a new strategy and algorithm that finds the embryo cell and recognizes inner structures of the cell, such as nucleus, polar body and zona pellucida.

Although the high magnification ratio of the optical microscope allows us precise visual information of the target object, however, higher magnification images also brings narrower filed-of-view and consequently it reduces the possible working area, spends more time in finding the objects.

Here, the new strategy means that the operator views multiple images that have the same viewpoint but have multiple magnification ratios. In the lower magnification image, he extracts the ROI (region of interest) area of the cell from the image acquired by using large viewing field. Then, the higher magnification image is used to recognize inner structures of the cell. Utilizing those multiple images increases the efficiency and the precision of biomanipulation.

Because the cell is alive and staying in the culture fluid, the conventional vision algorithms such as template matching and mathematical morphology operation are not useful in recognizing inner the structure of the cells [5-6]. Moreover, the several factors such as diverse size and shape of living cells and optical characteristic of the culture fluid make it difficult to recognize inner structure of the cell accurately.

It is found that the deformable template matching method is the better choice. We define first two deformable templates for the nucleus and polar body for a cell. And the calculated value of the energy function for each template will determine whether it is best fit or not. The deformable template and the energy function allow us to recognize accurate position of inner structure of the cell.

In section 2, our biomanipulation system is described. The proposed strategy and algorithm for recognizing the embryo cell is discussed in section 3 and section 4. Result of experiments is shown in section 5. Finally, in section 6, we summarize and discuss about the future study.

2. Biomanipulation System

A vision based biomanipulation system normally consists of three parts: first, an optical stereomicroscope with three CCD cameras mounted on stereomicroscope, secondly, the micro XY stage and micromanipulator for holding pipette and injection pipette, and thirdly, a PC with controller for micro XY stage, micromanipulator and image processing board. Fig. 1 shows the vision based biomanipulation system and its architecture.

The system contains an optical stereomicroscope with three magnification ratios (x400, x600 and x1200). So, we can get multiple images simultaneously. The micro XY stage is

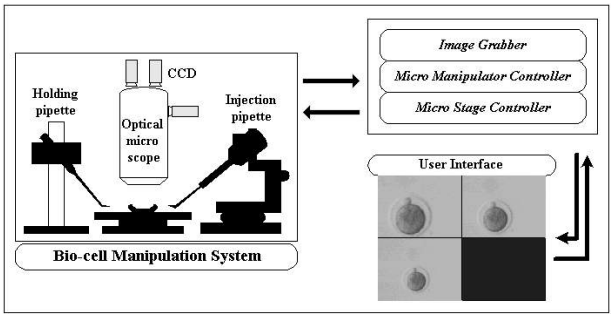

Fig. 1. An overview of the biomanipulation system

leadscrew-driven for translation moving with a travel range of 25mm. Precision crossed roller bearings guarantee straightness of travel of better than 2um. It uses a compact closed loop DC motor with a shaft-mounted high-resolution position encoder, and the precision gearhead provides 0.1um minimum incremental motion with a resolution of 0.0085um. The injection pipette and holding pipette are installed on the micromanipulator with 3DOF (Degree Of Freedom), actuated by three stepping motors. The position of each axis (x,y,z) is measured by the encoder. The mobile range of each xyz axis is 25.4mm and the step resolution of the stepping motor is 0.04um.

3. Biomanipulation strategy

In this section, we describe the cell recognition strategy and its merit of using the multiple magnification images [7].

3.1 Multiple Images

As the magnified image provides more precise view, it is natural that such image contains better information of the target cells. However, the highly magnified image brings also narrower visual field. Moreover, any slight movement of holding or injection pipette conveys a large displacement in the highly magnified image. On the other hand, since the less magnified image shows a wide area, one can find the cell within the image rapidly, and ignore small amount of displacement error. However, the lower resolution of less magnified image makes it difficult to recognize exact position of inner structures of the cell. Fig. 2 shows FOV (field of view) of highly magnified and less magnified images,

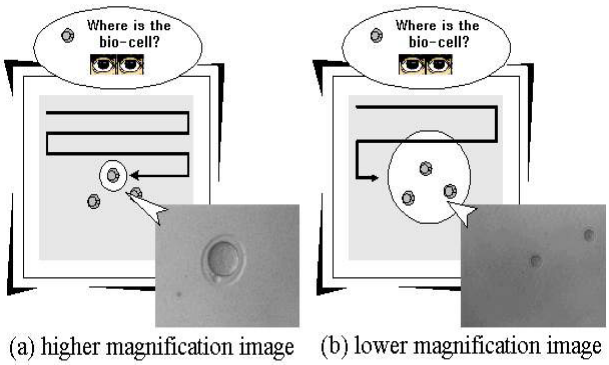

Fig. 2. FOV (field of view) of higher and lower magnification image

respectively. The former provides a more detail information about inner structure of the cell than the latter.

3.2 A strategy based on multiple images

The use of those multiple images increases efficiency and precision of biomanipulation.

Fig. 3 shows the user interface for a strategy based on multiple images. Three windows show images that have magnification ratio of 400, 600 and 1200, respectively. First, the system extracts the ROI area within an image with a magnification ratio of 400 by using histogram segmentation algorithm. When the system succeeds in extracting the ROI area of the cell, it generates a moving trajectory to the center of the image by moving the micro XY stage using visual feedback.

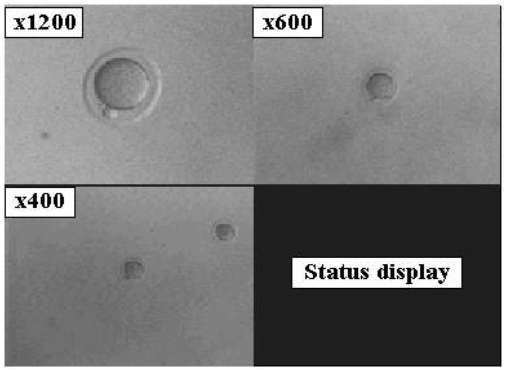

Fig. 3. User interface

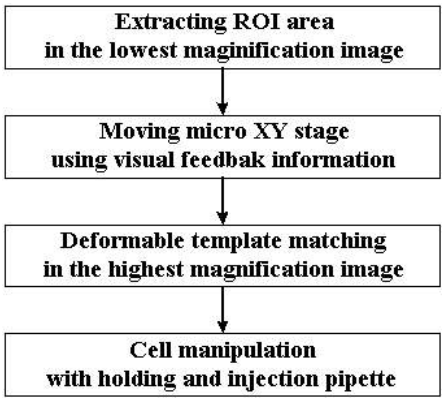

Fig. 4. Biomanipulation strategy

Then, it starts to search about the inner structures of the cell. However, if it fails, it regards that cell as an irregular cell. Fig. 4 shows a flowchart of the biomanipulation strategy.

4. Bio-cell recognition

Our target cell here is the mouse embryo. It is widely used for biomanipulation because of its similarity to the human embryo. Fig. 5 shows the structure of a mouse embryo, consisting of nucleus, polar body and zona pellucida. The arrow A shows the insertion position of the injection pipette. It is necessary to prevent any destruction of the polar body during insertion of the injection pipette into the embryo. Therefore, it is essential

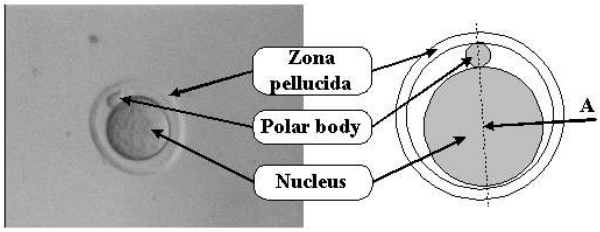

Fig. 5. The structure of a mouse embryo

to recognize the exact positions of the nucleus and the polar body.

The present recognition algorithm is composed of two parts: the ROI area extraction and the cell recognition part. In this section, we discuss the bio cell recognition algorithm.

4.1 Extraction of the ROI area

To recognize the structure of the cell, first of all, we need to extract the ROI area of the cell from the given image. Such preprocess operation increases the eventual recognition rate and reduces the computational time by applying deformable template matching only to the ROI area by selection. The present preprocess operations consists of histogram segmentation and the nearest neighborhood method [9].

Fig. 6 shows an image of the mouse embryo cells and a histogram for the image. Since the background area occupies the most area of the image, the neighborhood of the peak in the histogram corresponds to the background area of the image ('a' point in Fig. 6). By using this characteristic, we can easily eliminate the background area. Indeed, Fig. 7 shows the result image after eliminating the neighborhood area of the peak.

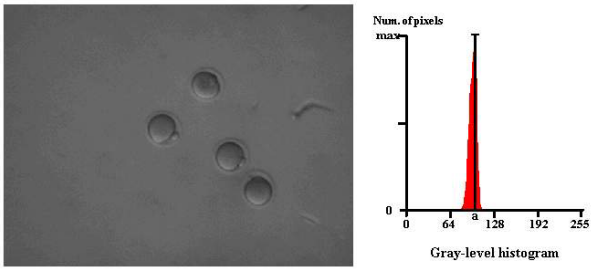

Fig. 6. An image of the mouse embryos and its histogram

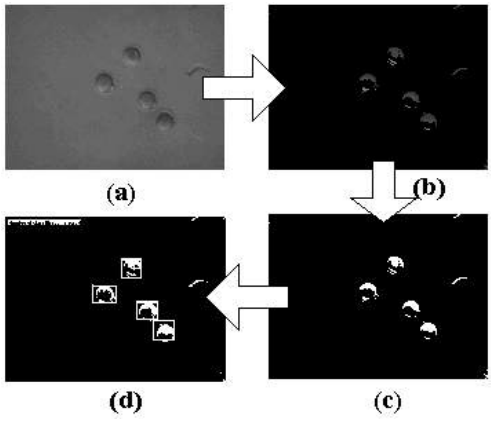

Fig. 7. Steps of extracting the ROI area

Fig. 7 illustrates several steps how the ROI area can be extracted from the given gray image. Once the background gray pixels are removed from the image, the image becomes Fig. 7(b). After digitization of that image, each cell area consists of a group of white pixels as shown in Fig. 7(c). What we need here is grouping of those pixels according to their geometrical distance between them. The algorithm based upon the nearest neighborhood clustering is used for classifying the groups of white pixels. The algorithm finds the nearest pair of distinct clusters and merges the pair of clusters. The result image is shown in Fig. 7 (d).

4.2 Deformable template matching

The deformable template matching models a target object using a template with a few parameters [8, 10]. By doing so, it recognizes the target object within a given image by adjusting the parameters. Although one can have a complex deformable template using many parameters, then the search time will increase rapidly. Therefore the complexity of a deformable template model must trade off between the search time and the recognition accuracy.

To simplify our task, we made three assumptions:

(1) Shape of the nucleus is similar to a circle.
(2) Shape of the polar body is similar to an ellipse.
(3) The nucleus and the polar body do not overlap each other.

4.2.1 Deformable template of nucleus

Fig. 8 shows a deformable template for the nucleus. It has three parameters, x , y and r , corresponding to two coordinates of the center and the radius of the template, respectively. Three parameters are selected for modeling the nucleus according to the assumptions (1).

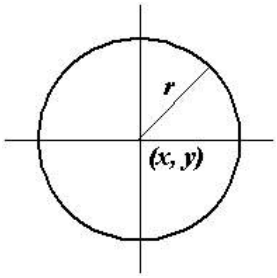

Fig. 8. The deformable template for the circular nucleus

An arbitrary point on the template is defined as $p(x, y)$. From that point, the upper and lower contours are given by

$$\begin{aligned} &\textit{Upper contour } p(x,y) = \left\{ x \in [-r, r] \,|\, y = \sqrt{r^2 - x^2} \right\} \\ &\textit{Lower contour } p(x,y) = \left\{ x \in [-r, r] \,|\, y = -\sqrt{r^2 - x^2} \right\} \end{aligned} \quad (1)$$

4.2.2 Deformable template for the polar body

Fig. 9 shows the deformable template for the polar body of the mouse embryo. To model this template, we need the left and right half circles and two lines connecting two half circles.

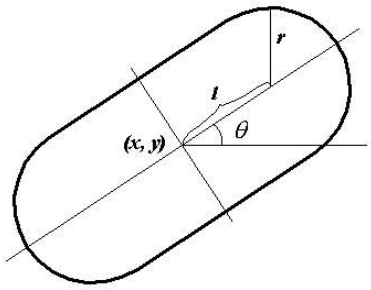

Fig. 9. Deformable template for the polar body

Hence, there are five parameters, x , y , l , r and θ , corresponding to two coordinates for the center, the length from the center of the template to the center of the half circle, the radius of the half circle and the rotational degree of the template.

We define an arbitrary point on the upper straight line which connects two half circle as follow

$$\begin{aligned} &p_{ul}(x,y): x \in [-l,l] \\ &x = x\cos\theta + (y+r)\sin\theta \\ &y = -x\sin\theta + (y+r)\cos\theta \end{aligned} \tag{2}$$

where p_{ul} is an arbitrary point on the upper straight line. And an arbitrary point on the lower straight line, p_{ll} is defined as follow

$$\begin{aligned} &p_{ll}(x,y): x \in [-l,l] \\ &x = x\cos\theta + (y-r)\sin\theta \\ &y = -x\sin\theta + (y-r)\cos\theta \end{aligned} \tag{3}$$

Another arbitrary point on the left half circle, p_{lc} is defined as follow

$$\begin{aligned} &p_{lc}(x,y): x \in [-r,r] \\ &x' = -\sqrt{r^2 - y^2} \\ &x = (x'-l)\cos\theta + y\sin\theta \\ &y = -(x'-l)\sin\theta + y\cos\theta \end{aligned} \tag{4}$$

The final arbitrary point on the right half circle, p_{rc} is defined as follow

$$\begin{aligned} &p_{rc}(x,y): x \in [-r,r] \\ &x' = \sqrt{r^2 - y^2} \\ &x = (x'+l)\cos\theta + y\sin\theta \\ &y = -(x'+l)\sin\theta + y\cos\theta \end{aligned} \tag{5}$$

4.2.3 Energy function

To decide whether the ROI area is a nucleus or not, an energy function is introduced. The energy function is defined as shown in (6). Here, as the template models the nucleus accurately, the energy function becomes larger.

$$E_{total} = E_{edge} + E_{deviation} \tag{6}$$

The energy function consists of two terms: the edge enhancement term E_{edge} and the deviation term $E_{deviation}$. The first term is an integration of the coordinates on the template contour

$$E_{edge} = \frac{1}{255n}\sum_{i=0}^{n}\phi_{edge}^{i}(x,y) \tag{7}$$

where n is the number of pixels on the template contour and potential field ϕ_{edge} is the edge enhanced image by using Sobel operator. Fig. 10 illustrates potential field ϕ_{edge} of an image of the mouse embryo cells.

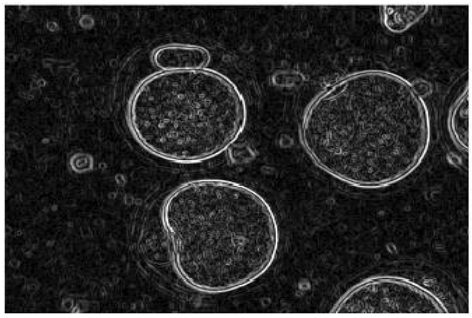

Fig. 10. The edge potential field

In fig. 10, one can observe a lot of noise even after applying the noise elimination filter. Since such noise decreases the recognition rate, a deviation term is adopted. By using the deviation term, we can increase the recognition rate and stability of the energy function. The deviation term $E_{deviation}$ is given by:

$$E_{deviation} = 1 - \frac{1}{255}\sqrt{\frac{1}{n}\sum_{i=1}^{n}(ave - \phi_{edge}^{i}(x,y))^2} \tag{8}$$

where ave is an average of the coordinate on the template contour.

4.2.4 The search strategy

Given that the processing time is critical in the biomanipulation system, we have designed a dynamic search area algorithm. This algorithm is able to change the search area dynamically. Fig. 11 illustrates the concept of dynamic search area algorithm.

Fig. 11 shows the search area of the deformable template of the nucleus as well as the polar body. If the center of the template $p(x,y)$ is outside the area A, the location of the template is out of the search area. So, the search area is restricted by radius r . In case of the nucleus, we define

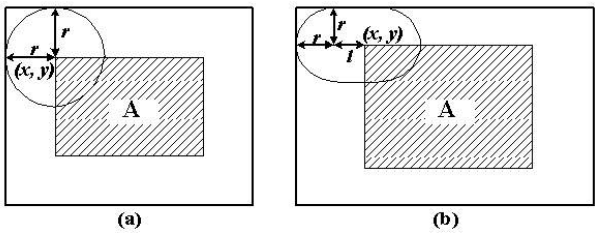

Fig. 11. Concept of the dynamic search area algorithm

interval of radius r as follow

$$l_s \times \frac{1}{2} \times 0.9 \le r \le l_s \times \frac{1}{2} \tag{9}$$

where l_s is the length of minor axis of the ROI area. The interval of the center of the template $p(x,y)$ is defined as follow

$$\begin{aligned} r \le x \le l_l - r \\ r \le y \le l_s - r \end{aligned} \tag{10}$$

where l_l is the length of the major axis of the ROI area.

In case of the polar body, the interval of the radius r is defined as follow

$$(l_l \times 0.175) \times 0.25 \le r \le l_l \times 0.175 \tag{11}$$

And the interval of the center of the template $p(x,y)$ the rotational degree of the template θ is defined as follow

$$\begin{aligned} r+l \le x \le l_l - (r+l) \\ r+l \le y \le l_s - (r+l) \\ \theta' - 20 \le \theta \le \theta' + 20 \end{aligned} \tag{12}$$

where θ' is the rotational degree of the orthogonal line, which connect the center of the nucleus and the polar body.

5. Experiments

We construct an embryo cell image database to verify the performance of the proposed bio cell recognition algorithm. The database is made by biomanipulation system discussed in section 2 and includes 138 mouse embryo images with 400, 600 and 1200 magnification ratio, respectively. Fig. 12 is a

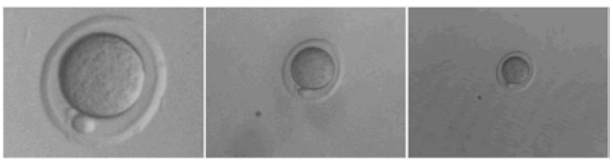

Fig. 12. Cell image database

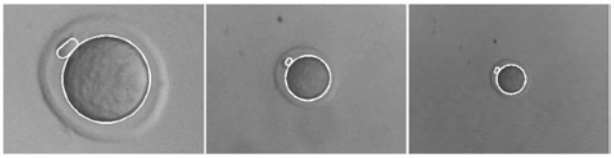

Fig. 13. Result images

part image of the database, and Fig. 13 shows the images of result after applying the proposed algorithm to the database

Fig. 13 illustrates the recognition of the cell's nucleus and polar body represented by two white circles, whereas Fig. 12 is the original images. Table 1 compares the result between the conventional mathematical morphology operation and the proposed algorithm. Only if the proposed algorithm recognizes nucleus and polar body simultaneously, we count it as a success case. The proposed algorithm took 65ms, 100ms and 450ms of the average processing time for each magnification ratio, respectively, and shows 52.2%, 80.4% and 93.5% of the average recognition rate, respectively, suggesting that the larger magnification, the longer the processing time although the recognition rate increases.

Table 1. Experimental result

Magnification ratio	x1200	x600	x400
Processing time	450ms	100ms	65ms
Recognition rate	93.5%	80.4%	52.2%

Result suggests that the proposed algorithm shows the higher recognition rate than the mathematical morphology operation. Moreover, it provides detail information on inner structure of the cell, despite that fact that it spends more time compared to the mathematical morphology operation.

To verify the proposed new cell recognition strategy, we accomplish serial operations, such as finding cells, moving them to the center of the image and recognizing inner structure of the cell. Our result shows that the total time of the operations was about 9 second.

Previous data suggest that an expert operator can manipulate about 13~14 units of cell for a day, because he feels eyestrain and looses concentration. On the other hand, the automatic biomanipulation system with the proposed strategy and algorithm can manipulate cells without any fatigue and losing any concentration, so it can manipulate more cells than manual biomanipulation in the long term.

6. Conclusions

For developing an automatic biomanipulation, we have designed a vision based biomanipulation system. We proposed a new strategy and algorithm for recognizing inner structure of the cell, such as nucleus, polar body, and zona pellucida. The strategy is to utilize multiple images that have same viewpoint but have multiple magnification ratio. So, we can find the cell in the petri dish and recognize the inner structure of the cell accurately. The main part of the algorithm consists of histogram segmentation and a deformable template matching.

For increasing recognition rate and reducing computational load, histogram segmentation and dynamic search area algorithm is proposed. And, two simplified deformable templates were defined to recognize nucleus and polar body of cell. Our result suggests that the proposed algorithm showed a high recognition rate.

Our future plan is to develop an algorithm for recognizing holding pipette and injection pipette. For automating biomanipulation, the recognition algorithm to control pipettes is asked.

References

[1] Sun Yu, and Bradley J. Nelson, "Microrobotics Cell Injection", Proc. of the 2001 IEEE ICRA, pp.620-625, 2001

[2] Fumihito Arai, Tomohiko Sugiyama, Poom Luangjarmekorn, Akiko Kawaji, Toshio Fukuda, Kouichi Itoigawa, and Atsushi Maeda, "3D Bio-Micromaniplation", 1999 International Symposium on Micromechatronics and Human Science, pp. 71-77, 1999

[3] Y.kimura, R. Yanagimachi, "Intracytoplasmic Sperm Injection in the Mouse", Biology of Reproduction, Vol. 52, No.4, pp.709-720, 1995

[4] Fumihito Arai, Akiko Kawaji, Poom Luangjarmekorn, Toshio Fukuda, and Kouichi Itogawa, "Three-Dimensional Bio-Micromanipulation Under the Microscope", Proc. of IEEE ICRA 2001, pp.604-609, 2001.

[5] Dwi Anoraganingrum, "Cell Segmentation With Median filter and Mathematical Morphology Operation", Image Analysis and Processing, 1999. Proc of International Conference on, pp.1043-1046, 1999

[6] Xudong Li, Guanghua Zong and Shusheng Bi, "Development of Global Vision System for Biological Automatic Micromanipulation System", Proc. of IEEE ICRA 2001, pp. 127-132, 2001.

[7] Seok Joo Lee, Kyunghwan Kim, Deok-Ho Kim, Jong-Oh Park, and Gwi Tae Park, "Multiple Magnification Image Based Micropositioning for 3D Micro Assembly", Proc. of ICARCV 2002, pp. , 2002.

[8] Gwan Soo Lee, "Automatic Face Region Detection Using Chromaticity Space and Deformable Template", Master's thesis, 2001.

[9] Gregory A. Baxes, "Digital Image Processing: Principles and Applications", John Wiley & Sons, Inc. 1994.

[10] A. L. Yuille, D.S. Cohen and P.W. Hallinan, "Feature Extraction from Faces Using Deformable Templates", Proc. CVPR, 1989